Semiclassical quantization of KAM resonances in time-periodic systems

1994 J. Phys. A: Math. Gen. 27 6579

(http://iopscience.iop.org/0305-4470/27/19/028)

J. Phys. A: Math Gen. 27 (1994) 6579–6604. Printed in the UK

Semiclassical quantization of KAM resonances in time-periodic systems

B Mirbach and H J Korsch

Fachbereich Physik, Universität Kaiserslautern, D-67663 Kaiserslautern, Germany

Received 25 February 1994, in final form 27 June 1994

Abstract. A semiclassical theory for the quasi-energy spectrum of time-periodic systems with accidental classical resonances is presented. The primitive EBK quantum conditions for integrable systems are extended to multiply periodic flux tubes occuring in resonant systems. Replacing classical actions by appropriate differential operators in a classical resonance Hamiltonian yields a uniform quantization of states related to a classical resonance region. The derivation being general for time-periodic systems unfolds the organization of the quasi-energy spectrum, reducing it to the spectrum of a single time-independent Hamiltonian of one degree of freedom with additional rational shifts of $\hbar\omega$. In a first-order approximation the resonance Hamiltonian is reduced to a pendulum leading to a differential equation of the Mathieu type for the quasi-energies. It is rigorously shown how parameters of the differential equation can be drawn from classical dynamics, using the data of the 'essential' orbits in the resonance zone, i.e. stability coefficients and actions of hyperbolic and elliptic orbits as well as actions of homoclinic orbits. The quasi-energy spectrum of a forced quartic oscillator is studied numerically and evaluated. Semiclassical quasi-energies related to a resonance of period three are computed and compared with exact quantum mechanical eigenvalues.

1. Introduction

Extensive studies of dynamical systems during the last decades have shown that in generic Hamiltonian systems both regular and chaotic motion coexist. The complicated, but fascinating, phase-space structure of such systems has been inspected in great detail (see, e.g., [1, 2]), at least for two-dimensional systems. The usual approach is to consider a perturbed integrable Hamiltonian

$$H = H_0(I_1, I_2) + \epsilon H_1(I_1, I_2, \varphi_1, \varphi_2) \tag{1}$$

where $(I_1, I_2, \varphi_1, \varphi_2)$ denote the action-angle variables of the integrable system with Hamiltonian H_0. The phase space of the integrable system is entirely stratified by invariant tori specified by the actions I_1, I_2, which are constants of motion. The torus is parametrized by angles φ_1, φ_2 such that the motion on the torus is linear in time, i.e. $\varphi_i(t) = \omega_i t + \varphi_i(0), i = 1, 2$, with frequencies

$$\omega_i(I_1, I_2) = \frac{\partial H}{\partial I_i} \qquad i = 1, 2\,. \tag{2}$$

A resonance corresponds to commensurable frequencies (ω_1, ω_2) yielding a rational winding number, i.e. $\Omega = \omega_1/\omega_2 = r/s (r, s \in \mathbb{N})$.

The KAM theorem tells us that tori in the neighbourhood of a resonance r/s are usually destroyed. In a surface of section, one finds a chain of s islands embedded in a stochastic layer. The centres of the islands are elliptic fixed points as a result of the intersection of

0305-4470/94/196579+26$19.50

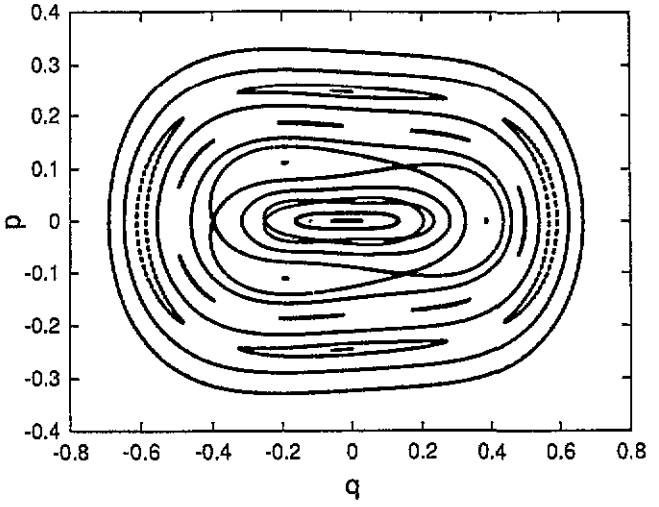

Figure 1. Stroboscopic Poincaré section for a driven quartic oscillator for weak driving force. The most prominent features are a period-three island chain and a chain of two period-two islands. Chaotic regions are very small.

an s-periodic stable orbit with the surface of section. In between, one finds s hyperbolic fixed points, whose homoclinic intersections generate the chaotic motion surrounding the islands. The area of this stochastic band depends on the perturbation strength ϵ and the denominator s of the frequency ratio (see, e.g., [1, 3]). Although the resonant tori are dense in phase space there remains—for sufficiently small ϵ—a finite phase space volume occupied by invariant tori since the width of the island chains declines sufficiently rapidly with its order s (a typical example are the Poincaré intersections shown in figure 1). As a consequence, these resonances can be considered as isolated in the limit of small ϵ.

A description of the motion in the vicinity of a resonance is achieved by transformation to a rotating coordinate frame [1]. In this way the global resonant motion is separated from the slow relative motion, which allows for an adiabatic treatment.

A first integrable approximation is obtained by averaging over the fast variable. As a result, one is left with a one-dimensional (time-independent) Hamiltonian which is periodic in the remaining angle variable with period $2\pi/s$. Especially for weak perturbations, this Hamiltonian is that of the pendulum [1, 4, 5], also referred to as the 'standard Hamiltonian' because it is generic, i.e. it appears typically in KAM systems independent of the particular Hamiltonian. The phase space in the vicinity of a resonance exhibits two types of motion, namely stable libration around elliptic fixed points and rotational motion above and below the islands separated by separatrix branches from the librational motion.

The influence of isolated classical resonances on the energy spectrum has been studied by a number of authors. Avoided crossings, e.g. those which typically show up in plots of the eigenvalue spectrum versus a perturbation parameter, are related to isolated resonances in the classical dynamics [6–9]. Primitive quantization rules for multiply periodic resonant flux tubes were presented [6, 7, 10–12] as well as uniform methods which allow for a continuation of the semiclassical quantization across the separatrix. Degeneracies, which might appear in primitive quantization due to discrete symmetries, are removed in this way and one obtains splittings of energy levels due to dynamical tunnelling [13] between resonant tori.

Among other techniques, one method based on classical resonance theory is the replacement of the actions in the resonance Hamiltonian by differential operators [14, 6, 7]. This uniform method seems to provide the best physical insight into the interrelation between isolated resonances and the energy spectrum and had been successfully applied in the study

of avoided crossings.

Whereas these studies are all concerned with coupled oscillator systems, the present work will be devoted to time-periodic systems. By introducing an extended phase space, time-periodic Hamiltonian systems in one dimension can be treated as two-dimensional autonomous systems. Within this approach they form a particular subclass of two-dimensional systems. Therefore, quantization rules for time-periodic systems can be drawn from the well known EBK rules for autonomous systems as demonstrated by Breuer and Holthaus [15]. Bensch *et al* [16] developed a quantization method based on Poincaré surfaces of section, which allows us to perform the quantization in two independent steps, in contrast to related methods for general two-dimensional systems. As we will show when briefly recapitulating this quantization theory in section 2, this is due to a separation of the classical quasi-energy function in the quantizing action variables.

After a short overview of classical resonance theory in section 3, we will present a theory of the quasi-energy spectrum based on a semiclassical quantization of the resonance Hamiltonian. The basic ansatz for a uniform quantization is a replacement of the actions in the resonant Hamiltonian by differential operators in essentially the same way as done by Ozorio [7] and Uzer *et al* [6] in their studies of coupled oscillator systems.

For the class of time-periodic systems, however, it will turn out that the quasi-energy spectrum can be reduced to the spectrum of a time-independent Hamiltonian with one degree of freedom. Additional rational shifts of $\hbar\omega$, which are due to the boundary conditions in the rotating coordinate frame, then reproduce the quasi-energy spectrum of the original Hamiltonian. As a result, we obtain a general organization scheme of the quasi-energy spectrum in the vicinity of a classical resonance.

In the pendulum approximation, also referred to as 'centre-of-resonance approximation' by other authors, uniform quantization leads to an eigenvalue equation of Mathieu form. In section 4, we derive expressions for the parameters of the Mathieu equation in terms of classical phase-space data and show how these data can be drawn from classical dynamics, independent of the underlying system.

Uzer *et al* [6] had a similar idea to use data of the separatrix and additional quantized tori in order to predict the level splittings. Here we propose a different method, namely to use the data of the stable and unstable periodic orbit in addition to those of the separatrix. The separatrix data can be obtained from the action difference of homoclinic orbits and the unstable periodic orbit [17, 18]. This allows the extension of the method to the generic case of non-isolated resonances disturbing each other so that the separatrix does not join smoothly any more but generates homoclinic intersections, which are the onset of a chaotic layer around the resonant islands.

Moreover, in this way a step is made towards Gutzwiller's trace formula [19]. Within this quantization theory, the energy eigenvalues appear as singularities in a sum over all periodic orbits, with the consequence that one needs, in principle, all periodic orbits in order to determine any eigenvalue precisely. This theory works very successfully for systems exhibiting hard chaos, i.e. systems allowing for a coding of periodic orbits such that only a few of them are necessary for quantization. For mixed systems, however, the Gutzwiller theory seems to be hard to apply.

We will show how the uniform quantization, being based on the generic resonant dynamics, allows us to compute eigenvalues by using the data of the 'essential' classical orbits in the resonance zone.

In section 5, we derive the primitive EBK quantization rules for resonant flux tubes based on geometric path considerations. Within this approach, the quasi-energy states localized on secondary tori inside the resonance reveal a very transparent structure representing the

limiting case where dynamical tunnelling between the tori is negligible.

As an illustrative example we evaluate the quasi-energy spectrum of a periodically driven Duffing oscillator and compute explicitly quasi-energies related to a resonance of period three.

2. *Quantization of time-periodic systems*

One way to achieve a semiclassical quantization of one-dimensional time-periodic systems is to increase the dimension by constructing an extended phase space in which the system appears to be time-independent, so that the EBK quantum conditions

$$I_i = \frac{1}{2\pi}\oint_{\gamma_i} p\cdot \mathrm{d}q = \hbar\left(n_i + \tfrac{1}{4}\mu_i\right) \qquad n_i \in \mathbb{Z} \qquad i = 1,\ldots,N \tag{3}$$

for two-dimensional autonomous systems can be implemented. A comprehensive description of this theory can be found in [15, 16]. Here, we give only a brief outline as far as necessary for the theory presented in the subsequent sections.

By regarding t as a variable and introducing a conjugate canonical momentum p_t, a new conserved Hamiltonian $\widetilde{H}$, the quasi-energy function, is obtained:

$$\widetilde{H}(p, q, p_t, t) = H(p, q, t) + p_t\,. \tag{4}$$

Invariant surfaces in extended phase space $\{p, q, p_t, t\}$ are topologically not two-dimensional tori but non-compact cylinders. In the case of a time-periodic system, however, one can regard t as an angle variable by identifying t and $t+T$ with the corresponding frequency $\omega = 2\pi/T$ being the constant driving frequency. In this way, the invariant cylinders form connected tori allowing for an implementation of quantum conditions (3). The natural choice of a surface of section is the plain defined by $\{t = 0 \bmod T\}$. We choose the loop γ_1 lying in this plane, whereas γ_2 is chosen as a path connecting a point (p, q) at time $t = 0$ with the same point at time $t+T$. After solving (4) for p_t on the quasi-energy shell $\varepsilon = \widetilde{H}(q, p, t, p_t) = \text{constant}$, quantization conditions (3) adopt the form

$$\begin{aligned} I_1 &= \frac{1}{2\pi}\int_{\gamma_1}\omega^1 = \hbar\left(n_1 + \tfrac{1}{4}\mu_1\right) \qquad n_1 \in \mathbb{Z} \\ I_2 &= \frac{1}{2\pi}\int_{\gamma_2}\omega^1 + \frac{T}{2\pi}\varepsilon = \hbar n_2 \qquad n_2 \in \mathbb{Z} \end{aligned} \tag{5}$$

with the Poincaré–Cartan form $\omega^1 = p\,\mathrm{d}q - H\mathrm{d}t$. No Maslov index appears in the quantum condition for I_2 since there is no turning point in the time direction, i.e. it is always possible to choose γ_2 such that $\mu_2 = 0$.

The quantization can be performed in two steps. The quantization condition for I_1 has to be fulfilled first, and the second condition in (5) determines the value of the quasi-energy yielding the typical Brillouin zone structure of the quasi-energy spectrum:

$$\varepsilon_{n_1,n_2} = -\frac{1}{T}\int_{\gamma_2}\omega^1 + \hbar\omega n_2\,. \tag{6}$$

In a preceding article [16] the quasi-energy function was rewritten as

$$\widetilde{H} = \omega_1 I_1 + \omega_2 I_2 - \langle L\rangle \tag{7}$$

by transforming the integral over γ_2 into a repeated integral over γ_1 and a path following a classical trajectory. Here, ω_i $(i = 1, 2)$ are the frequencies of the angle variables corresponding to the two actions, where the latter one is the constant driving frequency,

i.e. $\omega_2 = \omega$, and $\langle L \rangle$ is the torus average of the Lagrangian which can also be written (and computed in practice) as the long-time average

$$\langle L \rangle = \lim_{m\to\infty} \frac{1}{mT} \int_0^{mT} L(q, \dot{q}, t)\, \mathrm{d}t\,. \tag{8}$$

Equation (7) is also valid in the more general case of two-dimensional autonomous systems. For one-dimensional time-periodic systems, however, $\langle L \rangle$ is a function of I_1 alone, such that the dependence of the quasi-energy function on the actions separates as

$$\tilde{H} = h(I_1) + \omega I_2\,. \tag{9}$$

This is the formal reason why the quantization can be performed in two separated steps as stated above. Inserting the quantization conditions (5) into (7) finally yields

$$\varepsilon_{n_1,n_2} = \hbar\omega\big(n_2 + \Omega\big(n_1 + \tfrac{1}{4}\mu\big)\big) - \langle L \rangle \tag{10}$$

with frequency ratio $\Omega = \omega_1/\omega$.

These quasi-energies are the eigenvalues of the quantum Hamiltonian $\hat{\tilde{H}}(q,t) = \hat{H}(q,t) - \mathrm{i}\hbar\partial_t$ with time-periodic eigensolutions (note that p_t in (4) has been replaced by the differential operator of the conjugate variable, the time)

$$\big(\hat{H}(q,t) - \mathrm{i}\hbar\partial_t\big)u_{n_1,n_2} = \varepsilon_{n_1,n_2}u_{n_1,n_2}\,. \tag{11}$$

The transition operators for a ladder of periodic solutions $\{u_{n_1,n_2},\ n_2 \in \mathbb{Z}\}$ are $a^{\pm} = \mathrm{e}^{\pm\mathrm{i}\omega t}$, i.e. the solutions can be written as

$$u_{n_1,n_2}(t) = u_{n_1}(t)\mathrm{e}^{\mathrm{i}n_2\omega t} \tag{12}$$

with $u_{n_1} = u_{n_1,0}$. Consequently, the solutions of the time-dependent Schrödinger equation can be represented as

$$\Phi_{n_1}(t) = \mathrm{e}^{-\mathrm{i}\varepsilon_{n_1}t/\hbar}\, u_{n_1}(t) \tag{13}$$

which is the well known Floquet form and the traditional way of introducing the concept of quasi-energies [20, 21]. In this picture, the Brillouin zone structure of the quasi-energy spectrum appears as an ambiguity since each ladder of quasi-energies $\{\varepsilon_{n_1,n_2},\ n_2 \in \mathbb{Z}\}$ corresponds to a single solution Φ_{n_1} only.

3. Quantization of resonant dynamics

3.1. Classical resonance theory

Classically, a description of the generic resonant motion with rational winding number $\Omega = r/s$ can be achieved by transforming the system to a rotating coordinate frame followed by an adiabatic treatment. A comprehensive description of this method can be found in the book by Lichtenberg and Lieberman [1]. Here, we will only sketch it briefly and show how this transformation can be translated into quantum mechanics. The starting point is the transformation to a coordinate frame rotating with the resonance frequency $\omega_1 = \omega_2 r/s$. The 'time'-coordinate φ_2 is kept and a new variable φ_1' is introduced, which measures the slow deviation from resonance

$$\varphi_1' = \varphi_1 - \frac{r}{s}\varphi_2 \qquad \varphi_2' = \varphi_2 \tag{14}$$

with generating function

$$F_2 = \left(\varphi_1 - \frac{r}{s}\varphi_2\right)I_1' + \varphi_2 I_2' \tag{15}$$

yielding the transformation of the actions

$$I_1 = I_1' \qquad I_2 = I_2' - \frac{r}{s} I_1' . \tag{16}$$

The next step is to expand the perturbational Hamiltonian H_1 in a Fourier series

$$H_1 = \sum_{m,n} H_{m,n} e^{i(m\varphi_1 + n\varphi_2)} \tag{17}$$

$$= \sum_{m,n} H_{m,n} e^{i(m\varphi_1' + (mr/s+n)\varphi_2')} . \tag{18}$$

An integrable approximation to the Hamiltonian is then obtained by averaging over the fast variable φ_2' yielding

$$\bar{H}_1 = \sum_{m=0}^{\infty} H_{-mr,ms} e^{ims\varphi_1'} . \tag{19}$$

This approximation is valid near the resonance, where $|\dot{\varphi}_2| \gg |\dot{\varphi}_1|$. Since the averaged Hamiltonian

$$\bar{H}(I_1', I_2', \varphi_1') = H_0(I_1', I_2') + \epsilon \bar{H}_1(I_1', I_2', \varphi_1') \tag{20}$$

is independent of φ_2', the action I_2' is a constant of motion, the first term of a series expansion for an adiabatic invariant of Hamiltonian (1). In this way, the dynamics generated by the Hamiltonian is reduced to an integrable motion in a single degree of freedom Hamiltonian specified by the action I_2. This Hamiltonian is periodic in the remaining angle variable φ_1' with period $2\pi/s$. It should be noted that this periodicity is independent of the perturbation! The next step in a perturbative treatment of the resonant motion is to expand the Hamiltonian (19) in the action I_1' around the resonant value. This will be described in section 5 with its implications on quantization.

3.2. Quantization of the resonance Hamiltonian

The primitive semiclassical quantization conditions for the actions in the rotating system can be easily obtained by inserting the conditions for the original actions (5) into the transformation (16), yielding

$$\begin{aligned} I_1' &= \hbar\left(n_1 + \tfrac{1}{4}\mu_1\right) \\ I_2' &= \hbar\left(n_2 + \frac{r}{s}\left(n_1 + \tfrac{1}{4}\mu_1\right)\right) \qquad n_1, n_2 \in \mathbb{Z} . \end{aligned} \tag{21}$$

For the sequel it will be more convenient to separate multiples of s from the first quantum number n_1 and absorb it into the second one, n_2, i.e. we introduce the pair of integers ($m \in \mathbb{Z}$, $l = 1, \ldots, s$), uniquely defined by $n_1 = sm + l$, rather than n_1 as quantum numbers. The quantization rules (5) then adopt the form

$$I_1' = \hbar\left(l + ms + \tfrac{1}{4}\mu_1\right) \tag{22}$$

$$I_2' = \hbar\left(n_2 + \frac{r}{s}\left(l + \tfrac{1}{4}\mu_1\right)\right) \qquad m, n_2 \in \mathbb{Z} \qquad l = 1, \ldots, s . \tag{23}$$

The advantage of this representation is that the quantum condition (23) uniquely determines the numbers n_2 and l, whereas the quantum number m is not affected.

These primitive semiclassical quantization rules, however, cannot be applied in the resonance zone since primary tori specified by the action I_1' are missing inside the separatrix. Quantization conditions for secondary tori, i.e. tori around the elliptic fixed points in the

resonance islands, will be derived in section 5 independent of the classical resonance theory, based only on geometrical path considerations.

As already realized by other authors [6, 7] a uniform quantization valid across the separatrix can be achieved by replacing the actions in the Hamiltonian by differential operators with respect to the corresponding angle variables. (For a more comprehensive presentation of action-angle variables in quantum mechanics see, for example, [22]).

If (I, φ) is any pair of action and angle variables, a pair of corresponding quantum operators $(\hat{I}, \hat{\varphi})$ fulfilling the commutator relation $[\hat{\varphi}, \hat{I}] = i\hbar$ is obtained by setting

$$\hat{I} = -i\hbar\partial_\varphi . \tag{24}$$

In order to recover the eigenvalues of the action operator correctly as specified by the related quantum condition $I_n = \hbar(n + \beta)$, one has to impose Bloch boundary conditions on the eigenstates $|n\rangle$ of $\hat{I}$, i.e.

$$\langle\varphi|n\rangle = \frac{1}{\sqrt{2\pi}} \exp(i(n + \beta)\varphi) . \tag{25}$$

An alternative, which allows for keeping periodic boundary conditions, is to redefine $\hat{I} = -i\hbar\partial_\varphi + \hbar\beta$ [14], but this advantage would be lost in the following.

Applying these rules to the actions (I_1', I_2'), the quantum conditions (22) and (23) imply

$$\langle\varphi_1'|m, l\rangle = \frac{1}{\sqrt{2\pi}} \exp\left(i\left(l + ms + \tfrac{1}{4}\mu_1\right)\varphi_1'\right) \tag{26}$$

$$\langle\varphi_2'|n_2, l\rangle = \frac{1}{\sqrt{2\pi}} \exp\left(i\left(n_2 + \frac{r}{s}\left(l + \tfrac{1}{4}\mu_1\right)\right)\varphi_2'\right) \tag{27}$$

for the eigenstates of the related action operators $\hat{I}_1'$ and $\hat{I}_2'$, respectively. Since the resonance Hamiltonian $\bar{H}$ in (20) is independent of φ_2', the quantum Hamiltonian $\hat{\bar{H}}$, obtained by replacing the actions (I_1', I_2') as described above, commutes with $\hat{I}_2'$. Consequently, each eigensolution $\Phi_{n_1,l,n_2}(\varphi_1', \varphi_2')$ of $\hat{\bar{H}}$ factorizes into an eigenstate $\langle\varphi_2'|n_2, l\rangle$ of $\hat{I}_2'$ and a one-dimensional function $\phi_{n_1,l}(\varphi_1')$, which is a linear combination of the eigenstates $\langle\varphi_1'|m, l\rangle$ of $\hat{I}_1'$ with l fixed according to (23):

$$\phi_{n_1,l}(\varphi_1') = \frac{1}{\sqrt{2\pi}} \exp\left(i\left(l + \tfrac{1}{4}\mu_1\right)\varphi_1'\right) \sum_m c_m \exp(ims\varphi_1') . \tag{28}$$

The functions $\phi_{n_1,l}$, $n_1 \in \mathbb{Z}$ are eigenfunctions of the one-degree of freedom Hamiltonian $\hat{\bar{H}}_{l,n_2}(\hat{I}_1, \varphi_1')$, the restriction of $\hat{\bar{H}}$ on the corresponding eigenspace $|n_2, l\rangle$ of $\hat{I}_2'$. This Hamiltonian is obtained when specifying the action I_2' according to quantum condition (23) and then replacing the remaining coordinates (I_1', φ_1') by the corresponding quantum operators. Since $\hat{\bar{H}}_{l,n_2}$ is periodic in φ_1' with period $2\pi/s$ it couples only those Fourier components with indices differing by multiples of s. This is the reason why the eigenfunctions adopt the special form (28) (see also [7]).

More generally speaking, the spectrum of $\hat{\bar{H}}_{l,n_2}$ has a band structure due to the periodicity in φ_1'. In our notation, the quantum number n_1 indicates the band and $l = 1, \ldots, s$ counts the states in the band. In general, however, this spectrum depends on the action I_2'. Moreover, the quantum number l is determined by quantum condition (23). In this way, the quantization condition for I_2' selects a series of states one from each band.

The two-dimensional eigensolution finally adopts the form

$$\Phi_{n_1,l,n_2}(\varphi_1', \varphi_2') = \frac{1}{2\pi} \exp\left(i\left(n_2 + \frac{r}{s}\left(l + \tfrac{1}{4}\mu_1\right)\right)\varphi_2'\right) \exp\left(i\left(l + \tfrac{1}{4}\mu_1\right)\varphi_1'\right) \sum_m c_j \exp(ims\varphi_1') . \tag{29}$$

By inserting the coordinate transformation (14), one can easily verify that this function fulfils the Bloch boundary conditions in the original angle variables φ_1, φ_2, as implied by the quantum condition (5) for I_1 and I_2.

3.3. Time-periodic systems

So far our treatment is general for two-dimensional autonomous systems with rotational motion in one direction. Now we specialize to the particular case of one-dimensional time-periodic systems. As shown in section 2 the quasi-energy function $\tilde{H}_0$ of an integrable time-periodic system written in action-angle variables has the particular form $\tilde{H}_0 = h(I_1) + \omega I_2$. Thereby, the action I_1 is a function of (p, q, t) alone (see (5)), whereas I_2 depends on the momentum p_t canonical conjugate to time. The perturbation $H_1(p, q, t)$ does not depend on I_2, due to this construction of the action variables and the resulting integrable approximation (20) to the quasi-energy function has the form

$$\tilde{H}(I_1, I_2, \varphi_1, \varphi_2) = h(I_1) + \epsilon H_1(I_1, \varphi_1, \varphi_2) + \omega I_2 \tag{30}$$

$$= h(I_1') + \epsilon H_1'(I_1', \varphi_1', \varphi_2') + \omega I_2' - \frac{r}{s}\omega I_1' . \tag{31}$$

After averaging over the fast variable φ_2', one is again left with a separable Hamiltonian

$$\bar{\tilde{H}}(I_1', I_2', \varphi_1') = h(I_1') - \frac{r}{s}\omega I_1' + \epsilon \bar{H}_1'(I_1', \varphi_1') + \omega I_2' =: H_{\mathrm{int}}(I_1', \varphi_1') + \omega I_2' . \tag{32}$$

Consequently, the quasi-energies of the corresponding quantum Hamiltonian are superpositions of two independent terms. If $E_{n_1,l}$ are the eigenvalues of $\hat{H}_{\mathrm{int}}$, we find, after inserting (23),

$$\varepsilon_{n_1,l,n_2} = E_{n_1,l} + \hbar\omega\frac{r}{s}\left(l + \tfrac{1}{4}\mu_1\right) + \hbar\omega n_2 . \tag{33}$$

In this way, the quasi-energy spectrum is reduced to the band spectrum of a single (!) one-degree of freedom Hamiltonian with additional rational shifts of $\hbar\omega$. Besides the Brillouin zone structure generated by the term $\hbar\omega n_2$, one finds a global energy shift $\hbar\omega\mu_1 r/4s$ in the case that the global motion is not rotational ($\mu_1 \neq 0$). Moreover, the s states $l = 1, \ldots, s$ in each band are shifted by $\hbar\omega l r/s$. These shifts by multiples of $\hbar\omega/s$ are due to the boundary conditions in the rotating coordinate frame and may not be mixed up with splittings in the energies $E_{n_1,l}$ which superimpose the shifts of $\hbar\omega/s$ in the quasi-energy spectrum. In the case of s degenerate energies $E_{n_1,l}$ in a band n_1 one finds an equidistant series of quasi-energies with spacing $\hbar\omega/s$, giving the impression of a 'finer' Brillouin zone structure.

The splittings of the states in a band of an s-periodic potential can be understood as a result of tunnelling through the barriers of the potential. This physical interpretation is provided by a uniform WKB theory, which is obtained by considering complex-valued action integrals through potential barriers and applying matrix techniques [23, 24]. Within this semiclassical theory approximate formulae for the width of energy gaps and energy bands have been derived.

We recommend here, in particular, the work by Connor *et al* [24], where, in addition to a general theory for $2\pi/s$-periodic potentials, a detailed analysis of the particular case of the Mathieu equation can be found. This equation is of special interest in the context of dynamical resonances, as will become clear in the following section.

For a given problem it might be hard to find the analytic form of the integrable approximation H_{int} to the Hamiltonian. This is, however, not the intention of the present work. We rather want to show how—independent of the underlying system—data drawn from the actual classical dynamics can be used to compute quasi-energies and to understand the influence of a classical resonance on the quasi-energy spectrum in detail.

4. The pendulum approximation

As shown in textbooks of dynamics (see, e.g., [1, 5]), the integrable approximation of the resonant Hamiltonian is a 'pendulum' for sufficiently small perturbation. This result is derived in two steps. First, it is argued that the Fourier amplitudes in (19) generally fall off exponentially with the order m such that it is sufficient to use terms up to first order:

$$\bar{H} = H_0 + \epsilon H_{0,0} + 2\epsilon H_{-r,s} \cos s\varphi_1' \,. \tag{34}$$

Here, the origin of the angle φ_1' has been chosen such that the fixed-point positions defined by $\partial \bar{H}/\partial \varphi'_1 = 0$ are located at $\varphi'_{1,0} = 0$ and π/s for elliptic and hyperbolic fixed points, respectively. In addition, there are s copies of each of these fixed points at positions shifted by multiples of $2\pi/s$. The next step is to expand this Hamiltonian in I_1' about the value $I'_{1,0}$ fulfilling the resonance condition, i.e.

$$\left.\frac{\partial H_0}{\partial \varphi_1'}\right|_{I'_{1,0}} = \frac{\partial H_0}{\partial \varphi_1} - \frac{r}{s}\frac{\partial H_0}{\partial \varphi_2} = \omega_1 - \frac{r}{s}\omega_2 = 0 \,. \tag{35}$$

In lowest order, $I'_{1,0}$ is thus the location of the fixed points in the action direction. Since $\mathrm{d}I_1'/\mathrm{d}t = \mathrm{o}(\epsilon)$, an expansion in I_1' corresponds to an expansion in ϵ of the same order. Expanding H_0 to second order in $\Delta I_1' = I_1' - I'_{1,0}$ and keeping the lowest-order term in ϵ and $\Delta I_1'$, one obtains

$$\bar{H} = E_0(I'_{1,0}) + G(\Delta I_1')^2/2 - F\cos s\varphi_1' \tag{36}$$

with

$$E_0(I'_{1,0}) = H_0' + \epsilon H_{0,0} \tag{37}$$

$$G(I'_{1,0}) = \left.\frac{\partial^2 H_0'}{\partial I_1'^2}\right|_{I'_{1,0}} \tag{38}$$

$$F(I'_{1,0}) = \epsilon H_{-r,s}(I'_{1,0}) \,. \tag{39}$$

In general, these parameters implicitly depend on the second action I_2', which has to be specified by the quantization condition (23). The Hamiltonian $\bar{H}$ in (34) is that of a pendulum, however, depending on $s\varphi_1'$ rather than φ_1'. By rescaling the angle φ_1' this difference to the usual pendulum can be removed. For the quantum treatment, however, this would require an adjustment in the Bloch boundary conditions. To avoid this, we prefer to deal here with the Hamiltonian (36) as it stands. Hence, the phase space of this Hamiltonian consists of a band of s copies of the pendulum phase space (see, e.g., [1]).

One finds s elliptic fixed points located at $(\Delta I_1', \varphi_1') = (0, 0 + j2\pi/s)$, $j = 0, \ldots, s-1$, and s hyperbolic fixed points at positions shifted by π/s in the angle relative to those of the elliptic points. The librational motion around the elliptic fixed points is separated from the outer rotational motion by separatrices intersecting at the hyperbolic fixed points. It is convenient to introduce the parameters

$$R = (F/G)^{1/2} \qquad \text{and} \qquad \omega_0 = s(FG)^{1/2} \,. \tag{40}$$

The eigenvalues of the stability matrix are then found to be $\mathrm{e}^{\pm \mathrm{i}\omega_0 t}$ for the stable fixed point and $\mathrm{e}^{\pm\omega_0 t}$ for the unstable fixed point. This means that ω_0 appears both as the frequency for linear oscillations around the elliptic fixed points and as the positive stability exponent of the hyperbolic fixed point. The two separatrix branches are described by the formula

$$I_1'^{\pm}(\varphi_1') = \pm 2R\cos\left(\tfrac{1}{2}s\varphi_1'\right) + I'_{1,0} \,. \tag{41}$$

The 'size' of the resonance defined as the symplectic area enclosed by the two separatrix branches $I_1'^{\pm}(\varphi_1')$ is given by

$$A = A^+ - A^- = \int_{-\pi}^{\pi} (I_1'^{+}(\varphi) - I_1'^{-}(\varphi))\,\mathrm{d}\varphi = 16R\,. \tag{42}$$

Furthermore, the resonance is located at

$$I_{1,0}' = \frac{1}{4\pi}(A^+ + A^-)\,. \tag{43}$$

Within the uniform approximation as described in the previous section, the eigenvalues of the corresponding quantum Hamiltonian $\hat{\bar{H}}$ are obtained by inserting the action operator

$$\widehat{\Delta I_1'} = -\mathrm{i}\hbar\partial_{\varphi_1'} \tag{44}$$

into (36) and solving the resulting eigenvalue equation $\hat{\bar{H}}\varphi = E\varphi$, which can be written in the Mathieu form

$$\phi'' + (a - 2q\cos s\varphi_1')\phi = 0 \tag{45}$$

with

$$a = \frac{2sR}{\hbar^2\omega_0}(E - E_0(I_{1,0}')) \qquad \text{and} \qquad q = (R/\hbar)^2\,. \tag{46}$$

The boundary conditions for the solutions are (compare (28))

$$\phi_{n_1,l}(\varphi_1' + 2\pi/s) = \exp\bigl(\mathrm{i}\,2\pi\bigl(l + \tfrac{1}{4}\mu'\bigr)/s\bigr)\phi_{n_1,l}(\varphi_1') \tag{47}$$

with

$$\tfrac{1}{4}\mu' = \bigl(\tfrac{1}{4}\mu_1 + I_{1,0}'/\hbar\bigr) \bmod 1\,. \tag{48}$$

This—in general fractional—Maslov index μ' is obtained when the quantum condition (22) is expressed in terms of $\Delta I_1'$ rather than I_1'. The boundary condition (47) can be satisfied for the characteristic values $a_{n_1,l}$, where $n_1 = 0, 1, 2, \ldots$ is the band number. As is easily verified, shifts in the action by multiples of $\hbar$ do not affect the spectrum. They only shift the quantum number l. So we have taken $\frac{1}{4}\mu'$ modulo 1 in (48) without loss of generality.

The idea is to approximate the real system in the vicinity of a resonance by a pendulum in order to use the solutions of the resulting Mathieu equation, i.e. the pendulum eigensolutions, as approximations for the eigenvalues and eigenfunctions of the real Hamiltonian. The mapping of the eigenvalues includes, however, a semiclassical approximation due to the transformation to action-angle variables which is the starting point of the resonance theory. In the following, we show how the required parameters can be completely obtained from the classical dynamics. This is possible without performing a transformation to action-angle variables, since all data used are canonical invariants. One should keep in mind that the phase space of the real dynamics is four-dimensional, being reduced to three dimensions in the integrable approximation by averaging over the fast variable. What is mapped onto the two-dimensional pendulum phase space is not the full dynamics in three dimensions but the restriction on the subspace specified by quantization condition (22) for I_2.

There are four parameters which have to be determined. Two of them, the location $I_{1,0}'$ and the size A of the resonance, determine the Mathieu equation with the boundary conditions uniquely (see (42), (46) and (48)); the other two, the frequency ω_0 and the constant energy term $E_0(I_{1,0}')$, are needed to transform the characteristic values $a_{n_1,l}$ of the Mathieu equation into eigenvalues of the Hamiltonian (see equation (46)). In detail, our proposed method for determining these parameters from the classical dynamics works as follows.

- The determination of the areas A^+ and A^- below the upper and the lower separatrix, respectively, yields the position $I'_{1,0}$ (43) as well as the size A (42) of the resonance which determines the parameter R (22). If the system under consideration is integrable or the chaotic layer surrounding the separatrix is small, the areas can be obtained by computing upper and lower invariant tori very close to the separatrices. For generic KAM systems, this will not be possible because of the stochastic layer produced by the transversal intersections of the stable and unstable manifold. In this case the theory of MacKay *et al* [17, 18] can be applied showing that even for resonances, where the manifolds do not join smoothly building separatrices, an 'area' of the resonance can still be defined. This area is computed as the action difference between homoclinic orbits and the hyperbolic periodic orbit (see the appendix).
- The frequency ω_0 can be obtained by a stability analysis of either of the periodic orbits, i.e. computing the stability matrix and determining the stability exponents by diagonalization. This stability analysis also allows us to localize the fixed points precisely, which is a prerequisite for determining, in particular, the action of the orbits with high accuracy.
- The constant term $E_0(I'_{1,0})$ in (46) can be calculated by utilizing the invariance of integrals of the Poincaré–Cartan form along closed paths under canonical transformations. In the rotating coordinates we find for the action of the periodic orbits

$$\begin{aligned} S^{\pm}_{\mathrm{po}} &= \int_{\mathrm{po}} I'_1 \mathrm{d}\varphi'_1 + I'_2 \mathrm{d}\varphi'_2 - \bar{H}\,\mathrm{d}t \\ &= s(2\pi I'_2 - T\bar{H}^{\pm}_{\mathrm{po}}) \end{aligned} \tag{49}$$

  where $+$ and $-$ refers to the hyperbolic and elliptic orbit, respectively, and the period of the periodic orbit is sT with $T = 2\pi/\omega_2$. Relation (49) is valid in the integrable approximation where these periodic orbits appear as equilibria, i.e. φ'_1 is constant along them. Using the positions of the equilibria in (36) on the other hand yields

$$\bar{H}^{\pm}_{\mathrm{po}} = E_0(I'_{1,0}) \pm F\,. \tag{50}$$

  Inserting this result as well as the quantized values (23) for I'_2 into (49) one finally finds

$$E_0(I'_{1,0}) = \hbar\omega_2\left(n_2 + \frac{r}{s}\left(l + \tfrac{1}{4}\mu_1\right)\right) - (S^{\pm}_{\mathrm{po}}/sT \pm F)\,. \tag{51}$$

  The action of either of the periodic orbits can therefore be used for determining the constant energy $E_0(I'_{1,0})$. On the other hand, since (51) are two equations, $E_0(I'_{1,0})$ can be eliminated and the parameter F is obtained as action difference of the periodic orbits as an alternative to the method described above. One can also use this redundancy of information to check whether the pendulum approximation is applicable.

Now solving the first equation in (46) for E and inserting (51) we finally obtain for the energy eigenvalues

$$\varepsilon_{n_1,l,n_2} = -\frac{1}{sT}S^{\pm}_{\mathrm{po}} + \frac{\hbar\omega_0}{2s\sqrt{q}}(a_{n_1,l} \pm 2q) + \hbar\omega_2\left(n_2 + \frac{r}{s}\left(l + \tfrac{1}{4}\mu_1\right)\right) \tag{52}$$

where the $a_{n_1,l}$, $l = 1, \ldots, s$, $n_1 \in \mathbb{N}_0$ are the characteristic values of the Mathieu equation (45). Again, this result is valid, in general, for all two-dimensional autonomous systems which are rotational in one direction. Whereas in this general case the parameters of the Mathieu equation depend on the action I'_2, there is only a single Mathieu equation to be solved in the case of a time-periodic system. The frequency ω_2 is to be replaced by the driving frequency ω of the system. In practice, the Mathieu equation is solved by a continued

fraction ansatz for the Fourier coefficients, which is a straightforward generalization of the algorithm described in [25].

In this way we have found a semiclassical formula for the quasi-energies within the pendulum approximation, which uses as parameters the data of either of the periodic orbits and the size and location of the resonance, which can also be expressed by the actions of the hyperbolic and homoclinic orbits.

5. Quantum conditions for multiply-periodic flux tubes

In this section, we will generalize the EBK quantum conditions to multiply-periodic flux tubes. Similar results for particular resonances in coupled oscillator systems have already been presented by various authors [10, 6, 7]. Our treatment, however, will be general for all time-periodic systems.

The resulting quantization rules are applicable for resonance islands, which are large compared to h, such that quantizing tori inside the resonance islands exist. This can, in particular, be the case for larger perturbations where a resonance treatment, as described in the sections 3 and 4, becomes inaccurate. Resonance zones then start overlapping, giving rise to chaotic motion. Nevertheless, elliptic fixed points often remain stable even after resonances have overlapped, and one finds a stability island around them allowing for quantization.

Suppose we have an r/s resonance originating from the perturbation of a torus with Maslov indices $\mu_1 = 0$ or 2 and $\mu_2 = 0$, as is always the case for time-periodic systems. Each flux tube surrounding an elliptic orbit of period s will close after s periods, appearing as s cylindrical tubes connected in time, i.e. the stroboscopic Poincaré section at $t_n = nT$ cuts the tube of length sT in s pieces of length T. Although we will, for convenience, denote the angle parametrizing the torus in the direction transversal to the surface of section as 'time', the following construction is general for two-dimensional autonomous systems with Maslov index $\mu_2 = 0$. A generalization to different Maslov indices is straightforward.

Our basic ansatz is to write the Floquet state $u(t)$ as a sum over s states $v^{(j)}$,

$$u(t) = \sum_{j=1}^{s} v^{(j)}(t) \tag{53}$$

each of them being the EBK wavefunction of the corresponding cylindrical tube. Since the cylinders are cyclically connected in time, the requirement of periodicity of $u(t)$ leads to cyclic conditions for the s functions, i.e. $v^{(j)}(t+T) = v^{(j+1)}(t)$, $j = 1 \ldots s$. Hence the sum (53) can be rewritten as

$$u(t) = \sum_{j=1}^{s} v(t + jT) \tag{54}$$

where $v(t)$ is sT-periodic in time. Visually speaking, we have switched from a T-periodic picture, where the quantization manifold appears as s cylinders, to a sT-periodic picture where we see a tube of length sT (see figure 2). In this way, the problem of constructing the T-periodic wavefunction u is carried over to the construction of an EBK wavefunction v on this torus leading to quantization rules similar to (5). To obtain these quantization conditions we define two paths on the flux tube according to the case of a T-periodic tube, namely a path γ_1 describing a closed loop in the surface of section and a path γ_2 connecting a point on the torus with itself in time sT. In the T-periodic picture we can choose between s loops γ_1 in the surface of section corresponding to the s islands generated by the intersection of the torus, all of them enclosing the same area (see figure 2).

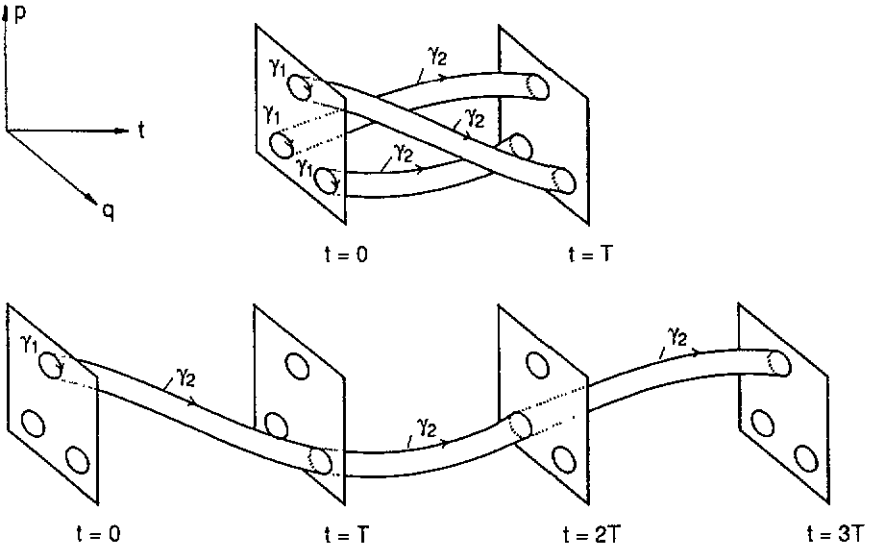

Figure 2. Resonant flux tubes surrounding an elliptic orbit of period three. The tubes are connected in time such that they form a single tube of length $3T$.

The quantization conditions are again derived from the uniqueness of the wavefunction along a closed loop. The wavefunction v (in the T-periodic picture the s functions $v^{(j)}$) have to be reproduced after going through the loop γ_1. Thus, the first quantization condition is identical to the ordinary one (5) for librational motion:

$$I_1 = \frac{1}{2\pi}\int_{\gamma_1} \omega^1 = \hbar\left(n_1 + \tfrac{1}{2}\right) \qquad n_1 \in \mathbb{N}_0 . \tag{55}$$

It should be noted, however, that the action I_1 along path γ_1 has nothing to do with the action variable used in subsection 2.4, and it is merely the form of the equation which coincides with (5); the path γ_1 is different.

The derivation of the second quantization condition requires more care. Although there are no turning points in time, and the path γ_2 hence has no folds in the time direction, the global motion of the flux tube itself can generate loops if it is twisted around a central periodic orbit. The path γ_2 has to follow this global motion, as sketched in figure 2. The rotational or librational character of the global motion is specified by a Maslov index μ_1, counting the number of folds on the original perturbed torus in the surface of section. In case of a r/s resonance, the flux tube of length s generates $r\mu_1$ folds, and the second quantization condition hence has the form

$$I_2' = \frac{1}{2\pi s}\int_{\gamma_2} p\,\mathrm{d}q + p_t\,\mathrm{d}t = \frac{\hbar}{s}\left(n_2' + \tfrac{1}{4}r\mu_1\right). \tag{56}$$

The number of loops can also be regarded as the number of times the path touches the—in general complicated—caustic generated by the dynamics on the flux tubes. Splitting up the quantum number into $n_2' = n_2 s + lr, l \in \{1, \ldots, s\}, n_2 \in \mathbb{Z}$, which is always possible if r and s are coprime, equation (56) coincides with the quantum condition (23) derived in subsection 3.2. Replacing p_t by $\varepsilon - H$ one obtains

$$\varepsilon_{n_1,l,n_2} = -\frac{1}{sT}\int_{\gamma_2} \omega^1 + \hbar\omega\frac{r}{s}\left(l + \tfrac{1}{4}\mu_1\right) + \hbar\omega n_2 \tag{57}$$

after solving the resulting equation for ε. Each quantizing torus, specified by the path γ_1 and indicated by n_1, provides a series of s equidistant quasi-energies with step size $\hbar\omega/s$. Comparing (57) with the result (33) one finds that this series of s states corresponds to s degenerate states in a band n_1 of the effective one-dimensional Hamiltonian with energy

$$E_{n_1,l} = E_{n_1} = -\frac{1}{sT}\int_{\gamma_2} \omega^1 \qquad l = 1, \ldots, s\,. \tag{58}$$

This is not surprising since we constructed the wavefunction as a superposition of s tube wavefunctions neglecting tunnelling between them. In general, however, the s energies $E_{n_1,l}$ will not be degenerate but show a level splitting which is due to dynamical tunnelling [13] between the s cylinders.

The practical computation of the energies is completely analogous to the case of T-periodic flux tubes, as described in section 2. The integral of the Poincaré–Cartan form is again transformed into an integral over the path γ_1 and a classical trajectory leading to

$$E_{n_1} = \hbar\omega_1\left(n_1 + \tfrac{1}{2}\right) - \langle L\rangle \tag{59}$$

where $\langle L\rangle$ is the Lagrangian average over the flux tube of length sT and the frequency ω_1 *is the winding number on the torus multiplied by the driving frequency.*

Writing the sT periodic wavefunction v as

$$v_{n_1,l,n_2}(t) = v_{n_1}(t)\mathrm{e}^{\mathrm{i}(lr/s+n_2)\omega t} \tag{60}$$

in analogy to (12), we find for the T-periodic Floquet solutions the expression

$$u_{n_1,l,n_2}(t) = \left(\sum_{j=1}^{s} v_{n_1}^{(j)}(t)\mathrm{e}^{\mathrm{i}2\pi jlr/s}\right)\mathrm{e}^{\mathrm{i}(lr/s+n_2)\omega t} \tag{61}$$

with $v_{n_1}^{(j)}(t) = v_{n_1}(t + jT)$ being the wavefunction of cylinder j. The solutions $\Phi_{n_1,l}(t) = \mathrm{e}^{-\mathrm{i}\varepsilon_{n_1,l,n_2}t/\hbar}u_{n_1,l,n_2}(t)$ of the time-dependent Schrödinger equation are then

$$\Phi_{n_1,l}(t) = \left(\sum_{j=1}^{s} v_{n_1}^{(j)}(t)\mathrm{e}^{\mathrm{i}2\pi jlr/s}\right)\mathrm{e}^{-\mathrm{i}E_{n_1}t/\hbar}\,. \tag{62}$$

Since these linear combinations are independent for different l, one can construct wavefunctions of the form

$$\Psi_{n_1}^{(j)}(t) = \mathrm{e}^{-\mathrm{i}E_{n_1}t/\hbar}v_{n_1}^{(j)}(t) \tag{63}$$

which are initially located on cylinder j and follow the flux tube in time.

6. Generalization to more than one island chain

Throughout the paper we have assumed, for convenience, that the island chain corresponding to the winding number $\Omega = r/s$ consists of s islands, which are cyclically connected with each other, which means that r and s are coprime. In general, however, there may be a number $k > 1$ of chains for a given winding number. This case can be included in our treatment by allowing r and s to not be coprime, i.e. $r = kr_0$, $s = ks_0$ with r_0, s_0 coprime, $k \in \mathbb{N}$. Then the total number of s islands can be divided into k groups (chains) of s_0 islands each, which are cyclically connected in time by k distinct closed flux tubes of period s_0. The appearance of more than one chain of islands is due to discrete phase-space symmetries which cannot be fulfilled by a single flux tube of period s_0 such that rather one finds a number k of such flux tubes which are related by discrete symmetry transformations [26].

The generalization of our semiclassical theory to this general case is straightforward. The starting point is the integrable approximation to the Hamiltonian which is still $2\pi/s$-periodic in the remaining angle variable (compare section 3). As before, this gives rise to the introduction of quantum numbers (n_1, l), where l runs over s states in each band n_1. What has to be modified in the final results are the rational shifts of $\hbar\omega$ which are added to the eigenvalues $E_{n_1,l}$ of the one degree of freedom Hamiltonian to yield the quasi-energies (see subsection 3.3). Splitting up l as $l = js_0 + l_0$, $j \in \mathbb{N}_0$, $l_0 = 1, \ldots, s_0$, equation (33) reads

$$\varepsilon_{n_1,l,n_2} = E_{n_1,l} + \hbar\omega\frac{r_0}{s_0}\left(l_0 + \tfrac{1}{4}\mu_1\right) + \hbar\omega n_2 . \tag{64}$$

The final equation (52) in section 5 has to be modified accordingly. By comparison with (33) one sees that actually only the common factor of k has been cancelled in the quotient r/s and the integer rj has been absorbed by n_2.

Rather than s distinct shifts of multiples of $\hbar\omega/s$ the shifts are only multiples of $\hbar\omega/s_0$, each of which appears k times in every band. The consequence is that—in the case of s-degenerate eigenvalues $E_{n_1,l}$—the quasi-energies are organized as an equidistant ladder of k-times degenerate states with step size $\hbar\omega/s_0$.

This organization scheme is also obtained from primitive torus quantization (section 5). The primitive quantization rules can be applied to any of the k (non-connected) flux tubes of period s_0 yielding an equidistant ladder of quasi-energies (compare (57) and (58))

$$\varepsilon_{n_1,l_0,n_2} = E_{n_1} + \hbar\omega\frac{r_0}{s_0}\left(l_0 + \tfrac{1}{4}\mu_1\right) + \hbar\omega n_2 \qquad l_0 = 1, \ldots, s_0 . \tag{65}$$

The k flux tubes are interrelated by symmetry transformations, and the semiclassical quantization yields k times the same result, leading to the structure described above.

The opposite extreme of the case $k = 1$ is the situation where $k = s$. Here we have s flux tubes of period one (not connected cylinders) which close after a single period. In this case one finds s degenerate quasi-energies without further rational shifts of $\hbar\omega$ since $s_0 = 1$.

Solutions of the Schrödinger equation, which fall in k distinct symmetry classes, are, in this primitive semiclassical context, independent linear combinations of the k semiclassical flux tube wavefunctions. In the real quantum system, one will find k almost degenerate states due to dynamical tunnelling. Each of these states belongs to a different symmetry class. As Bohigas *et al* [27] demonstrated, this property of states associated with flux tubes can be used to distinguish them from 'chaotic' states in a mixed system.

In the general case of k flux tubes of period s_0, one finds s_0 groups $l_0 = 1, \ldots, s_0$ of k almost degenerate states in different symmetry classes. The quasi-energies in different groups are shifted relative to each other by multiples of $\hbar\omega/s_0$ as expressed by (65).

Putting together the results, we conclude that each of the s quasi-energy states in one band is located on each of the s cylinders independent of the value of k. In the absence of tunnelling, a wavepacket initially located in one of the stability islands would follow the corresponding flux tube with period s_0, i.e. it would periodically show up in the s_0 islands of one chain similar to a classical wavepacket. In real quantum dynamics dynamical tunnelling to all of the s cylinders will occur, which gives rise to splittings in the energies $E_{n_1,l}$, $l = 1, \ldots, s$.

We emphasize again that the splittings appear in the quasi-energy spectrum only if the quasi-energies are taken modulo $\hbar\omega/s_0$.

7. An illustrative example

7.1. The classical model

As a model system we consider a forced quartic oscillator

$$H(t) = \frac{p^2}{2m} + \frac{bx^4}{4} - \lambda x \cos(\omega t) \,. \tag{66}$$

The system typically exhibits both regular and chaotic motion in coexistence, as predicted by the KAM theorem [16]. The Hamiltonian (66) depends on a single parameter (up to rescaling). Here we choose units with $m = b = \omega = 1$ and fix the remaining control parameter at $\lambda = 2 \times 3^{-4.5} \approx 0.014\,255\,6$. This particular choice of the force constant is due to Thylwe [28], who studied periodic orbits in the classical model. We adopt this parameter set since the phase space (see the Poincaré section in figure 1) shows rich resonant island structures without large chaotic zones. This means that the resonances disturb each other only slightly and can hencefore be treated as isolated. Furthermore, the smallness of the chaotic regimes avoids problems in performing primitive semiclassical torus quantization. The most prominent resonance structures are three connected island corresponding to winding number $\Omega = \frac{1}{3}$ and four islands (two pairs of connected islands) corresponding to $\Omega = \frac{1}{2}$.

7.2. Quasi-energies of the quantum Hamiltonian

Exact quantum computations of quasi-energies for Hamiltonian (66) were carried out using an Adams–Moulton predictor–corrector method [29] for $\hbar = 0.0005$. For this small value of $\hbar$ a sufficiently large number of states are localized in the dominant resonances such that primitive quantization on secondary, multiply periodic resonant flux tubes can be performed.

The quasi-energy states have been ordered according to increasing values of the expectation value of $\hat{H}$ at time zero and the number $\alpha = 0, 1, 2, \ldots$ counts the states in this ordering. In figure 3 the values of $\langle\alpha|\hat{H}(t=0)|\alpha\rangle$ are plotted versus α for the first 200

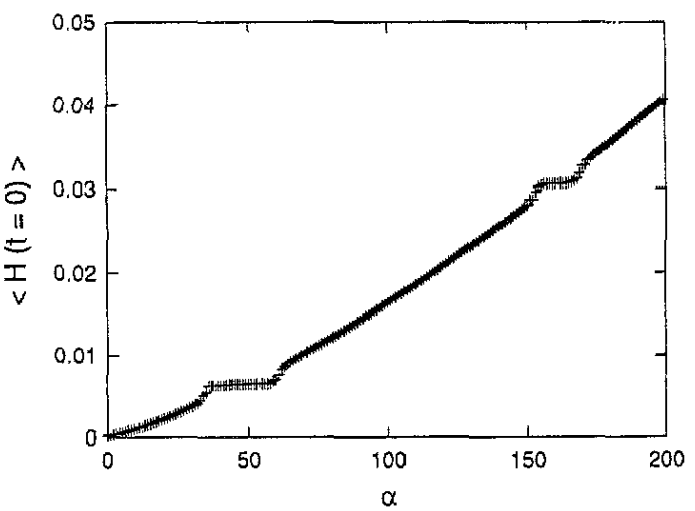

Figure 3. Expectation value $\langle\alpha|\hat{H}(t=0)|\alpha\rangle$ for a quasi-energy state α versus α. The plateaux correspond to classical resonances.

quasi-energy states. For high energies, where the oscillation is fast compared to the driving frequency ω, the classical energy $H(t)$ becomes an adiabatic constant of motion. Thus one expects at least for high energies (i.e. large values of α) the plot of $\langle\alpha|\hat{H}(t=0)|\alpha\rangle$ versus α to be approximately given by the classical function $H(t=0)(I)$, where I is the invariant of the (time-independent) system defined by Hamiltonian $H(t=0)$. But also for lower values of α the expectation value of the instantaneous Hamiltonian should—for a slightly disturbed system—give the correct ordering of the states in accordance with primitive quantization. This does, however, only apply to states allowing for primitive quantization on primary tori, outside the resonance regions.

For states semiclassically related to secondary tori inside the separatrix the expectation values $\langle\alpha|\hat{H}(t=0)|\alpha\rangle$ should lie in the range between the classical values of $H(t=0)$ on the unstable and stable fixed point, H^+ and H^-, respectively. Since these two values of $H(t=0)$ are close to each other, quasi-energy states related to a resonance form a plateau in the plot of the expectation values, clearly visible in figure 3. Here one recognizes two plateaus of quasi-energy states, which can be assigned to the large islands corresponding to winding numbers $\Omega = \frac{1}{3}$ and $\Omega = \frac{1}{2}$, respectively. For the particular case of the period-3 resonance, we found classical values of $H^+(t=0) = 6.97 \times 10^{-3}$ and $H^-(t=0) = 6.18 \times 10^{-3}$ which coincides precisely with the range of $\langle\hat{H}(t=0)\rangle$ covered by the corresponding plateau. Further plateaus corresponding to other, smaller, islands cannot be recognized.

In figure 4 the quasi-energy angle $\theta_\alpha = \varepsilon_\alpha T/\hbar$ is plotted versus α. Close to a resonance with winding number $\Omega = r/s$ primitive semiclassics tells us (see equation (10)) that adjacent quasi-energies differ approximately by

$$\varepsilon_{n_1+1,n_2} - \varepsilon_{n_1,n_2} \approx \hbar\omega r/s\,. \tag{67}$$

As a consequence, the quasi-energies appear to lie on s parallel equidistant branches having the shape of parabolas with the minima at the resonance centre. In figure 4 this structure appears most clearly for the resonance $\Omega = \frac{1}{2}$ at $\alpha \approx 160$. Moreover, one can recognize five parallel branches for $\alpha \approx 80$ and three for $\alpha \approx 50$, which show up less clearly. So far, this clear organization of the quasi-energies is to be expected for an integrable system even without resonance islands. The width of the parabolic parallel branches does not correspond

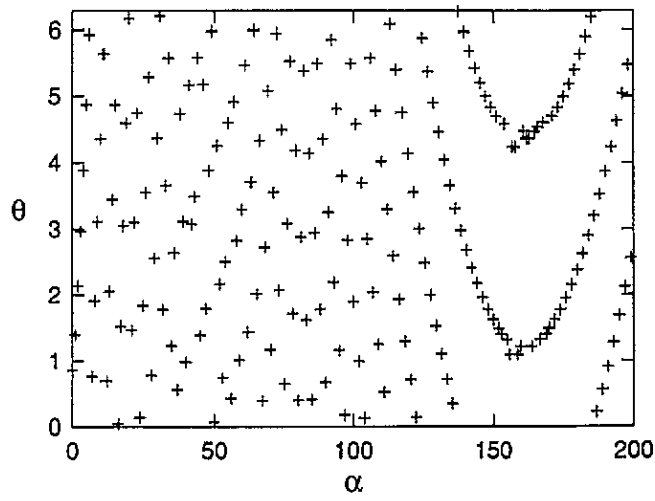

Figure 4. Quasi-energy angles $\theta_\alpha = T\varepsilon_\alpha/\hbar$ versus α for the first 200 quasi-energy states.

to the size of the classical resonance islands but is determined by the rate of change $d\Omega/dI$ of the winding number with the action, which is (up to a constant factor) the curvature of the parabola. In the present case this function declines with the action, leading to the broad structure corresponding to $\Omega = \frac{1}{2}$, in contrast to the smallness of the resonance islands.

The influence of the classical resonance islands on the quasi-energy spectrum manifests itself in deviations from these smooth curves, as is clearly visible for some quasi-energies at the minima of the two broad parabola. The number of states showing this deviation from the global trend is crudely determined by the area of the classical resonance. In the case of $\Omega = \frac{1}{3}$, the large resonance (again see figure 1) destroys almost completely the clear organization of the quasi-energies on parabolic curves.

7.3. Quasi-energies related to a period-3 resonance

In the following we analyse the quasi-energies in the vicinity of the period-3 island in more detail. Figure 5 shows the first 100 quasi-energy angles $\theta_\alpha = \varepsilon_\alpha T/\hbar$ plotted versus α as in figure 4. This time, however, the quasi-energy angles were taken modulo $2\pi/3$ such that the distribution of the states on the three parallel branches disappears and the typical structure of the quasi-energies spectrum turns out much more transparently, as already suggested by the theoretical considerations in the previous sections.

Connecting the states as ordered by α, one finds the quasi-energy angles lying on a smooth curve with slope $\sigma(\alpha) = 2\pi(\Omega(\alpha) - \frac{1}{3})$, where $\Omega(\alpha)$ is the winding number on the quantizing torus for state $|\alpha\rangle$. As discussed in the previous section, this ordering is in accordance with primitive semiclassical quantization and therefore breaks down on the separatrix. In our case we find the states up to $\alpha = 34$ and from $\alpha = 60$ upwards to fit into this scheme. In between, a different ordering scheme arranges the states in a series of triplets. This ordering can again be understood on the basis of primitive torus quantization, but, on secondary, period-3 flux tubes in the inner resonance islands as described in section 5. Therefore, we expect triplets of states degenerate modulo $2\pi/3$. Also, this ordering breaks down at the separatrix and one finds the triplets breaking up in their order from $n_1 = 6$

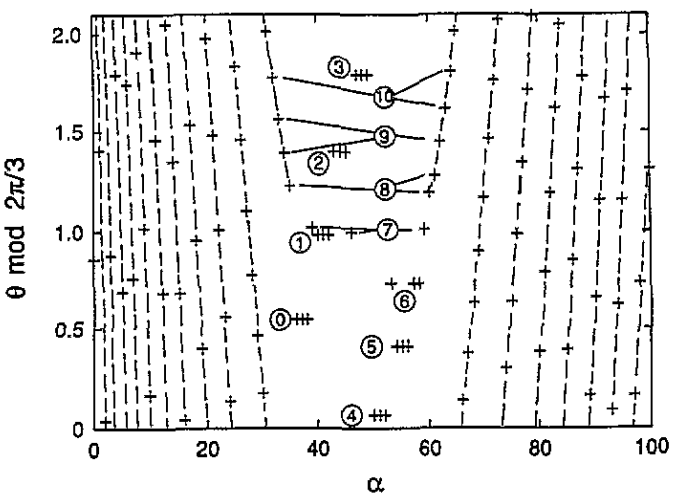

Figure 5. The first 100 quasi-energy angles θ_α taken modulo $2\pi/3$. Encircled numbers are the band numbers n_1 for a triplet of states connected by full lines. The broken lines connect states according to their α-ordering.

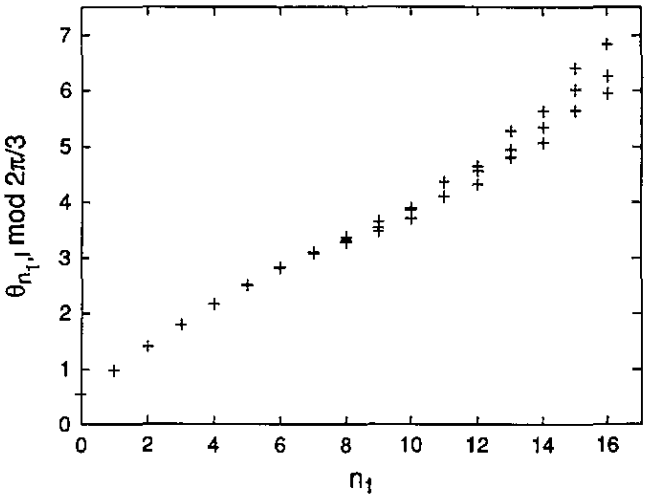

Figure 6. Quasi-energy angles $\theta_{n_1,l}$ modulo $2\pi/3$ versus band number n_1. An appropriate number of multiples of $2\pi/3$ has been added to the angles in order to make the systematic increase with n_1 visible.

upwards. For these states, the degeneration in the quasi-energies (taken modulo $2\pi/3$) also starts to split up. The encircled numbers in figure 5 combining three states are the band numbers n_1 (see sections 3 and 4) obtained from the uniform quantization, which will be described in more detail below. This ordering in bands of three states each can be continued across the separatrix, combining in an alternative manner two states above the separatrix with one below and vice versa. It should be noted that the band quantum numbers (n_1, l) cannot be assigned from the pure quantum computation.

Finally, in figure 6 the quasi-energy angles θ (again taken modulo $2\pi/3$) are plotted versus the band number n_1. In this plot both the global trend of the quasi-energies as well as the systematic increase of the splittings becomes clearly visible.

7.4. Primitive quantization

Now we turn to the semiclassical quantization which was a prerequisite for arranging the quasi-energies in bands, as shown above. First of all, one can estimate the number of states related to the resonance by enclosing the period-3 island as closely as possible by invariant tori. Such tori, approximating the resonance region from below and above, were found with areas (in units of $h = 2\pi\hbar \approx 0.003\,14$) of $A^- = 35.3$ and $A^+ = 61.1$, respectively. This yields an upper bound for the resonance area of $A_{\text{out}} = A^+ - A^- = 3 \times 8.6$. The largest period-3 torus we could find inside the resonance zone had an area of 8.3, yielding a lower estimation for the resonance area of $A_{\text{in}} = 3 \times 8.3$, which differs from the upper one by less than $\hbar$. According to the quantum condition $I_1 = \hbar\left(n_1 + \frac{1}{2}\right)$ (equation (55)) we conclude that nine bands $n_1 = 0, \ldots, 8$ should be related to the resonance region, where the band $n_1 = 8$ can be regarded as 'the' separatrix band, since the separatrix area is very close to the value of 3×8.5. Tori fulfilling the condition (55) for primitive quantization on secondary, three-periodic flux tubes, as described in section 5, can be found for $n_1 \leqslant 7$. Outside the resonance region, states with $\alpha \leqslant 34$ and $\alpha \geqslant 60$ allow for a primitive quantization on primary tori. The algorithm for performing the torus quantization is described in detail in [16], where it

is also shown how to include a first-order approximation to the quasi-energies in (10) in case the quantum condition for the action is not perfectly met. This approximation can also be used for extrapolating quasi-energies into chaotic regions from nearby tori. This was done in the present example for the states in band $n_1 = 8$, approximating the quasi-energies from both the inner and outer tori closest to the (slightly destroyed) separatrix.

7.5. *Uniform quantization of the approximate pendulum Hamiltonian*

As shown in section 4 one needs two parameters to determine the resulting Mathieu equation, namely location and size of the resonance. Although the tori provide a reasonable approximation for size and location of the resonances, an improvement is obtained when searching for homoclinic orbits and computing their action difference from the unstable orbit according to MacKay *et al* [18] (see appendix). The results for the area below the upper and lower separatrix are (in units of h) $A^+ = 61.09$ and $A^- = 35.41$, respectively, yielding a Maslov index (see (43) and (48)) of $\mu' = 3.0$ and the area determining the parameter q in the Mathieu equation (see (46) and (42)) is $A = A^+ - A^- = 25.68 = 3 \times 8.56$.

For transforming the characteristic values of the Mathieu equation into quasi-energies, one needs two further parameters which can be obtained from the data of one of the periodic orbits as shown in section 4. The actions of the periodic orbits were determined to be $S^+ = 77.57003\hbar$ and $S^- = 68.51471\hbar$. The winding number Ω of the stable orbit and stability exponent λ of the unstable one are $\Omega = 0.072\,19$ and $\lambda = 0.069\,56$. The noticeable difference between these two values indicates that the pendulum approximation is not perfect for the resonance under inspection. Since this resonance is quite extended in phase space in the radial direction, the 'centre-of-resonance approximation', i.e. the replacement of action-dependent parameters by their value at the resonance centre, is too crude.

Nevertheless, we choose this resonance as a testing case for our proposed method, in particular, since this resonance allows a primitive torus quantization very close to the separatrix, such that both methods can be compared with their different limitations.

Since only the data of one of the periodic orbits is required (again see (52)) we performed two independent computations using either of them. Note again that these two calculations correspond to identical characteristic values $a_{n_1,l}$ of the Mathieu equation (45) which are uniquely determined by location and size of the resonance. Action and stability exponent of the periodic orbit enter into the quasi-energies (52) as a constant and a factor, such that the results of the two different computations are simply related by an affine transformation. The splittings, in particular, are therefore proportional to ω_0 and independent of the choice of the action in (52) (see again (52)).

7.6. *Discussion*

The results of the different semiclassical quantizations schemes are presented in tables 1 and 2 for the bands $n_1 = 0, \ldots, 10$ together with the results of the quantum calculation. In table 2 quasi-energy angles are taken modulo $2\pi/3$ in order to remove shifts of $2\pi/3$, thus making the band splittings visible. Note that the assignment of quantum numbers (n_1, l) is due to uniform quantization. For bands up to $n_1 = 8$ they can also be assigned from the primitive quantization of the inner tori. The quantum numbers α can also be obtained from primitive quantization of outer tori (see the discussion in subsections 7.2 and 7.3); the values of α were put in parentheses where no quantizing tori exist.

As expected, the primitive quantization of the inner tori yields excellent results for

Table 1. Semiclassical quasi-energy angles $\theta_\alpha = \varepsilon_\alpha T/\hbar$ of primitive torus quantization and uniform quantization by using Mathieu solutions in comparison with exact quantum results. Quantum numbers α are put in parentheses where they cannot be obtained from primitive quantization on outer tori. Quasi-energies marked by '†' are obtained by extrapolation because the quantization condition could not be fullfilled within an error of $0.1\hbar$.

				Primitive semiclassical		Uniform semiclassical	
n_1	l	α	Exact	Inner	Outer	Stable	Unstable
0	1	(37)	0.5467	0.5477		0.5458	0.6191
0	2	(36)	2.6411	2.6420		2.6401	2.7135
0	3	(38)	4.7354	4.7365		4.7345	4.8078
1	1	(40)	0.9816	0.9826		0.9818	1.0391
1	2	(42)	3.0760	3.0770		3.0762	3.1336
1	3	(41)	5.1704	5.1714		5.1706	5.2280
2	1	(45)	1.3969	1.3984		1.3992	1.4414
2	2	(43)	3.4913	3.4928		3.4936	3.5358
2	3	(44)	5.5857	5.5872		5.5880	5.6302
3	1	(47)	1.7912	1.7919		1.7965	1.8243
3	2	(48)	3.8856	3.8863		3.8909	3.9187
3	3	(49)	5.9800	5.9807		5.9853	6.0131
4	1	(52)	2.1627	2.1646		2.1718	2.1859
4	2	(51)	4.2571	4.2589		4.2663	4.2803
4	3	(50)	0.0683	0.0702		0.0775	0.0915
5	1	(54)	2.5087	2.5111		2.5225	2.5238
5	2	(55)	4.6028	4.6055		4.6165	4.6178
5	3	(56)	0.4143	0.4167		0.4279	0.4292
6	1	(58)	2.8233	2.8283		2.8415	2.8311
6	2	(53)	0.7295	0.7339		0.7491	0.7387
6	3	(57)	4.9212	4.9227		4.9399	4.9294
7	1	(39)	3.1137	3.3372		3.1400	3.1187
7	2	(46)	5.1841	5.4316		5.2085	5.1882
7	3	(59)	1.0098	1.2428		1.0316	1.0109
8	1	60	3.2938	3.5061†	3.2188†	3.3214	3.2935
8	2	61	5.4723	5.6005†	5.4819	5.5044	5.4733
8	3	35	1.2333	1.4117†	1.1508†	1.2633	1.2341
9	1	33	3.6563		3.6545	3.6763	3.6356
9	2	34	5.5791		5.5626	5.6076	5.5727
9	3	62	1.4476		1.4369	1.4935	1.4560
10	1	32	3.7117		3.7050	3.7742	3.7298
10	2	64	5.9955		5.9918	6.0788	6.0268
10	3	65	1.7743		1.7671	1.7819	1.7339

the lower bands n_1, which show degenerate triplets when taken modulo $2\pi/3$. As this degeneration breaks up markedly, the deviations from the quantum results increase systematically from 1×10^{-3} for low values of n_1 to 2×10^{-1} for $n_1 = 7$ and 8.

For the results of the primitive quantization on primary tori outside of the separatrix, we find a corresponding increase of accuracy with n_1, i.e. when moving away from the separatrix.

As already mentioned above, one cannot—for the resonance under consideration—expect the uniform method to yield precise results for all quasi-energies, since the underlying

Table 2. Same data as in table 1, taken however modulo $2\pi/3$.

				Primitive semiclassical		*Uniform semiclassical*	
n_1	l	α	Exact	Inner	Outer	Stable	Unstable
0	1	(37)	0.5467	0.5477		0.5457	0.6191
0	2	(36)	0.5467	0.5477		0.5457	0.6191
0	3	(38)	0.5467	0.5477		0.5457	0.6191
1	1	(40)	0.9816	0.9826		0.9818	1.0392
1	2	(42)	0.9816	0.9826		0.9818	1.0392
1	3	(41)	0.9816	0.9826		0.9818	1.0392
2	1	(45)	1.3969	1.3984		1.3992	1.4414
2	2	(43)	1.3969	1.3984		1.3992	1.4414
2	3	(44)	1.3969	1.3984		1.3992	1.4414
3	1	(47)	1.7912	1.7919		1.7965	1.8243
3	2	(48)	1.7912	1.7919		1.7965	1.8243
3	3	(49)	1.7912	1.7919		1.7965	1.8243
4	1	(52)	0.0683	0.0702		0.0775	0.0915
4	2	(51)	0.0683	0.0702		0.0775	0.0915
4	3	(50)	0.0683	0.0702		0.0775	0.0915
5	1	(54)	0.4143	0.4167		0.4281	0.4294
5	2	(55)	0.4140	0.4167		0.4277	0.4290
5	3	(56)	0.4143	0.4167		0.4279	0.4292
6	1	(58)	0.7289	0.7339		0.7471	0.7367
6	2	(53)	0.7295	0.7339		0.7491	0.7387
6	3	(57)	0.7324	0.7339		0.7511	0.7406
7	1	(39)	1.0193	1.2428		1.0456	1.0243
7	2	(46)	0.9953	1.2428		1.0197	0.9994
7	3	(59)	1.0098	1.2428		1.0316	1.0109
8	1	60	1.1994	1.4117†	1.1244†	1.2270	
8	2	61	1.2835	1.4117†	1.2931	1.3156	1.2845
8	3	35	1.2333	1.4117†	1.1508†	1.2633	1.2341
9	1	33	1.5619		1.5601	1.5819	1.5412
9	2	34	1.3903		1.3738	1.4188	1.3839
9	3	62	1.4476		1.4369	1.4935	1.4560
10	1	32	1.6173		1.6106	1.6798	1.6354
10	2	64	1.8067		1.8030	1.8900	1.8380
10	3	65	1.7743		1.7671	1.7819	1.7339

pendulum approximation is too crude. However, using the data of the stable periodic orbit yields the quasi-energies in the lower bands, which are semiclassically localized on tori close to this fixed point, with the same accuracy as the primitive torus method ($\approx 1 \times 10^{-3}$). For higher bands the quasi-energies are overestimated when using this data set.

Using the data of the unstable fixed point instead, one finds the quasi-energies in high bands (in particular $n_1 = 7$ and 8) recovered with high accuracy, whereas those of low bands are markedly overestimated. Note, in particular, that the quasi-energies of band $n_1 = 8$—the state which is, according to our estimates of the resonance area, 'the separatrix state'—are predicted with the very high accuracy of 1×10^{-3}. This is the same limit of accuracy found in the primitive quantization of the degenerate states in the lower bands and seems therefore to be of inherently semiclassical origin for this model.

For states definitely outside of the resonance, i.e. $n_1 \geqslant 9$, the accuracy of the uniform

method declines with n_1. This is, however, the region where the primitive quantization (on primary tori) again works very well.

We conclude that the uniform quantization of the pendulum approximation yields very good results for states close to the separatrix ($n_1 = 7$ and 8) when using the data of the unstable periodic orbit and also in the case that the pendulum approximation is rather crude. The splittings of the quasi-energies are in any case obtained with high accuracy, since they are not very sensitive to the parameter chosen (they are, for example, independent of the action used in (52)). On the contrary, primitive quantization fails for these states since tunnelling has not been taken into account. But primitive quantization works very well where the uniform method based on the data of the unstable orbit becomes inaccurate, namely for states outside of the resonance and close to the stable orbit.

8. Concluding remarks

We have presented a uniform semiclassical theory of quasi-energies in the presence of accidental resonances based on essentially the same ideas as used by Uzer *et al* [6], Ozorio de Almeida [7], and other authors. Our presentation, however, is general and independent of the particular form of the action-angle variables in the unperturbed system. An application to one-dimensional time-periodic systems unfolds and explains the structure of the quasi-energy spectrum in the vicinity of a r/s-resonance, reducing it to the spectrum of a one-dimensional (time-independent) Hamiltonian of period $2\pi/s$ with additional shifts of integer multiples of $\hbar\omega/s$.

In a primitive torus quantization of secondary, multiply periodic flux tubes, the organization of the quasi-energy spectrum turns out most clearly yielding bands of quasi-energies which are degenerate modulo $\hbar\omega/s$. This primitive quantization represents the limiting case that dynamical tunnelling between the flux tubes is negligible.

Uniform approximations to the quasi-energies, which yield additional splittings of quasi-energies due to tunnelling, are obtained by mapping the resonant dynamics onto a pendulum and solving the resulting Mathieu equation for pendulum eigenstates. We have shown how the parameter of this equation can be obtained from classical dynamics, without any algebraic manipulations of the Hamiltonian. This makes our method applicable to a general class of systems. The confinement to systems which are rotational in one direction is only due to our interest in time-periodic systems, where the application of our results turns out nicely. The generalization to systems with Maslov indices $\mu_2 \neq 0$ is straightforward.

A determination of the relevant parameters is based on the data of the 'essential' orbits in the resonance zone, the stable and unstable periodic orbit as well as homoclinic orbits. This limited set of orbits is sufficient to compute all quasi-energies related to a classical resonance. Since this data set is redundant within the pendulum approximation one can also check the quality of the pendulum approximation based on these data. Moreover, we have demonstrated that even in the case that the pendulum approximation is rather crude, quasi-energies of 'separatrix-states' can be computed with high accuracy using the data of the unstable orbit.

A further step in a generalization of this method will be to use the redundant data to obtain two further coefficients in a higher-order expansion of the resonance Hamiltonian. This means taking into account further Fourier coefficients of the resonance Hamiltonian or expanding the Fourier coefficients to a higher order in the action. In any case, the derivation of the formulae for the additional coefficients in the resulting differential equation in terms of classical data is straightforward. The resulting differential equation, however, will be more general than the Mathieu equation.

An interesting option offered by the uniformization is a pertubational treatment of small resonances by utilizing an expansion of the characteristic values of the Mathieu equation in terms of the parameter q, which is given by the area of the resonance. Such a treatment, already presented by Voth [9] for the particular case of coupled oscillators, will shed light on the influence of small resonances on the quasi-energy spectrum, thus quantifying the naïve picture that resonance islands influence the spectrum only if their phase-space area is small compared to h. Such an analysis, however, has not been included in this work and will be published elsewhere.

A further interesting point is to test our method in the case that there is a chaotic layer around the (destroyed) separatrix which is larger than in the example studied here. The determination of resonance area and location by use of the action of homoclinic orbits as described in the appendix allows the application of the present semiclassical method to this case without further complications. Therefore one can study the influence of the destroyed separatrix on such states, in particular the transition to the case where the flux through the separatrix becomes larger than h.

Acknowledgments

We would particularly like to thank N Ben-Tal for carrying out the exact quantum computation, which was of essential importance for the present work. We also acknowledge stimulating discussions with K E Thylwe at the beginning of this work. This research has been supported by the Deutsche Forschungsgemeinschaft (Schwerpunktprogramm Atom- und Molekültheorie).

Appendix. Area below destroyed separatrix from action difference according to MacKay *et al* [17, 18]

Even for a destroyed separatrix, a resonance area can be defined by constructing a partial separatrix from segments of stable and unstable manifolds. These segments are joint in a homoclinic orbit, which approaches the unstable fixed point in both time directions. In general, there are two different homoclinic orbits, the so-called *minimum* orbit and the *minimax* orbit. The area under the partial separatrix differs according to the selection of the orbit in which the segments are joint. The difference between these two areas measures the flux through the destroyed separatrix (see the schematic illustration in figure A1). Note, however, that the area under the partial separatrix does not change under iteration; the flux through the separatrix is the same in both directions. MacKay *et al* [17] introduced the term *turnstile* to describe this motion through the separatrix. The turnstile is thereby formed by the two enclosed areas on both sides of the minimax orbit (see again figure A1).

Let $x_n^F, n = 1, \ldots, s$ be the iterates of the unstable fixed point under the Poincaré map, i.e. the intersections of the periodic orbit and x_n, $n \in \mathbb{Z}$, the iterates of the homoclinic point on the upper separatrix. This means that in the positive time direction the homoclinic point slides to the right on the stable manifold of the fixed point, i.e.

$$x_{i+js} \longrightarrow x_{i+1}^F \qquad j \to \infty \qquad i = 1, \ldots, s \tag{A1}$$

and slides to the left in the negative time direction on the unstable manifold:

$$x_{i+js} \longrightarrow x_i^F \qquad j \to -\infty \qquad i = 1, \ldots, s\,. \tag{A2}$$

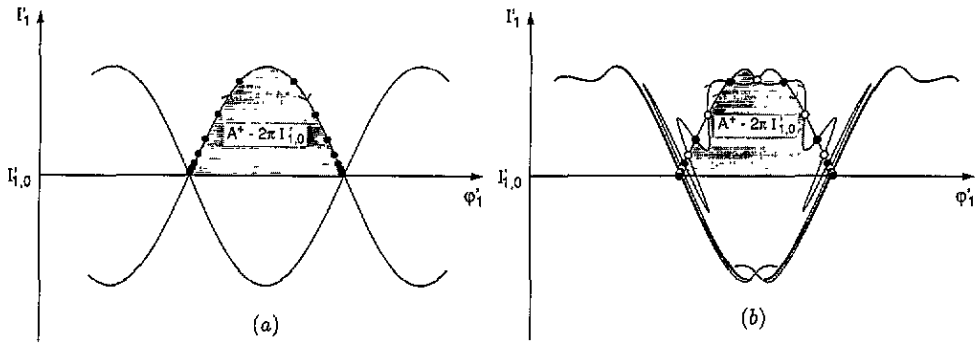

Figure A1. Phase-space area below separatrix branches. (*a*) A non-destroyed separatrix: branches of stable and unstable manifold are joined smoothly forming the separatrix. Any point of the separatrix is homoclinic to the unstable fixed point (example shown by dotted points). (*b*) Destroyed separatrix: branches of stable and unstable manifold intersect transversally, intersection points being homoclinic orbits. The resonance area (dark shaded) is given by the action difference between the unstable periodic orbit and the minimum homoclinic orbit (full circles) Flux through the destroyed separatrix (light-shaded area) is given as the action difference of the minimum and minimax (open circles) homoclinic orbit.

The integral

$$S(x_n, x_{n+1}) = \int_{nT}^{(n+1)T} L(x(t), \dot{x}(t), t)\,\mathrm{d}t \tag{A3}$$

of the Lagrangian L over one period along an orbit is the generating function for the Poincaré map, i.e.

$$p_n = \frac{\partial S(x_n, x_{n+1})}{\partial x_n} \qquad p_{n+1} = -\frac{\partial S(x_n, x_{n+1})}{\partial x_{n+1}}. \tag{A4}$$

Therefore, the integral $\int p\,\mathrm{d}q$ over a segment of the stable manifold can be rewritten as an infinite sum of action differences between iterates of the homoclinic point and the unstable fixed point. The result for the area below the separatrix, built by two segments as described above, is then an infinite sum

$$A^+ = s \sum_{j=-\infty}^{\infty} \sum_{i=1}^{s} \left(S(x_{js+i}, x_{js+i+1}) - S(x^{\mathrm{F}}_{js+i}, x^{\mathrm{F}}_{js+i+1}) \right) \tag{A5}$$

which converges exponentially fast. The expression for A^- is identical except for the sign, since the homoclinic orbit moves in the opposite direction.

In the practical computation, we followed the proposal of MacKay *et al* [18] to use a symmetry in the surface of section in order to reduce the problem of finding homoclinic orbits to a one-dimensional search problem. The 'minimax' orbit is, in general, lying on the symmetry line. Therefore one starts a point close to the fixed point and shifts it in the unstable direction until the point is lying on the symmetry line after a predetermined number j of iterations. This number of iterations is limited by the numerical accuracy and can be estimated from the instability of the orbit and the number of digits in the computation. However, since the sum (A5) converges exponentially with j, a small value of j is, in practice, sufficient; in our case the value of the action difference converges after about 30 periods.

The iterates of the second, the 'minimum' homoclinic orbits, are lying between those of the 'minimax' orbit. The 'minimum' homoclinic orbit has therefore no iterates on

the symmetry line, but is symmetric with respect to reflection on the symmetry line. It can therefore be found by a similar algorithm. The action difference between these two homoclinic orbits measures the flux through the (destroyed) separatrix. In the present case this action difference turns out to be negligible, which indicates that the separatrix is only slightly damaged, as already noticed.

For further detail we strongly advise the reader to study the work by MacKay *et al* [17, 18]

References

[1] Lichtenberg A J and Lieberman M A 1983 *Regular and Stochastic Motion* (New York: Springer)
[2] Tabor M 1989 *Chaos and Integrability in Nonlinear Dynamics* (New York: Wiley)
[3] Berry M V 1978 *Topics in Nonlinear Dynamics (Am. Inst. Phys. Conf. Proc.)* vol 46, ed S Jorna (reprinted in R S MacKay and J D Meiss 1987 *Hamiltonian Dynamical Systems* (Bristol: Hilger))
[4] Chirikov B V 1979 *Phys. Rep.* **52** 263
[5] de Almeida M O 1988 *Hamiltonian Systems—Chaos and Quantization* (Cambridge: Cambridge University Press)
[6] Uzer T, Noid D W and Marcus R A 1983 *J. Chem. Phys.* **79** 4412
[7] de Almeida A M O 1984 *J. Chem. Phys.* **88** 6139
[8] Voth G A and Marcus R A 1985 *J. Chem. Phys.* **82** 4064
[9] Voth G A 1986 *J. Phys. Chem.* **90** 3624
[10] Noid D W and Marcus R A 1977 *J. Chem. Phys.* **67** 559
[11] Martens C C and Ezra G S 1985 *J. Chem. Phys.* **83** 2990
[12] Martens C C and Ezra G S 1987 *J. Chem. Phys.* **86** 279; **87** 284
[13] Davis M J and Heller E J 1981 *J. Chem. Phys.* **75** 246
[14] Berry M V 1977 *Phil. Trans R. Soc.* **287** 237
[15] Breuer H P and Holthaus M 1991 *Ann. Phys., NY* **211** 249
[16] Bensch F, Korsch H J, Mirbach B and Ben-Tal N 1992 *J. Phys. A: Math. Gen.* **25** 6761
[17] MacKay R S, Meiss J D and Percival I C 1984 *Physica* **13D** 55 (reprinted in R S MacKay and J D Meiss 1987 *Hamiltonian Dynamical Systems* (Bristol: Hilger))
[18] MacKay R S, Meiss J D, and Percival I C 1987 *Physica* **27D** 1
[19] Gutzwiller M C 1990 *Chaos in Classical and Quantum Mechanics* (New York: Springer)
[20] Zel'dovitch Ya B 1967 *Sov. Phys.–JETP* **24** 1006
[21] Ritus V I 1967 *Sov. Phys.–JETP* **24** 1041
[22] Augustin S D and Rabitz H 1979 *J. Chem. Phys.* **71** 4956
[23] Child M S 1974 *J. Mol. Spectrosc.* **53** 280
[24] Connor J N L, Uzer T, and Marcus R A 1984 *J. Chem. Phys.* **80** 5095
[25] Abramowitz M and Stegun I A 1970 *Handbook of Mathematical Functions* (New York: Dover)
[26] Leopoldo J G, Percival I C, and Richards D 1982 *J. Phys. A: Math. Gen.* **64** 805
[27] Bohigas O, Tomsovic S, and Ullmo D 1990 *Phys. Rev. Lett.* **64** 1479
[28] Thylwe K-E 1993 *J. Sound Vib.* **161** 203
[29] Ben-Tal N, Moiseyev N, Leforestier C, and Kosloff R 1991 *J. Chem. Phys.* **47** 7311